

pubs.acs.org/Macromolecules Article

Benzo[1,2-b:4,5-b']dithiophenedimides as an Electron-Deficient Building Block for n-Type Polymer Semiconductors

Zhichun Shangguan, Zheng Yin, Cheng Li, Wansong Shang, Liangliang Chen, Chenying Gao, Xiang Xue, Xisha Zhang, Guanxin Zhang, and Deqing Zhang*



Cite This: *Macromolecules* 2024, 57, 6540–6547



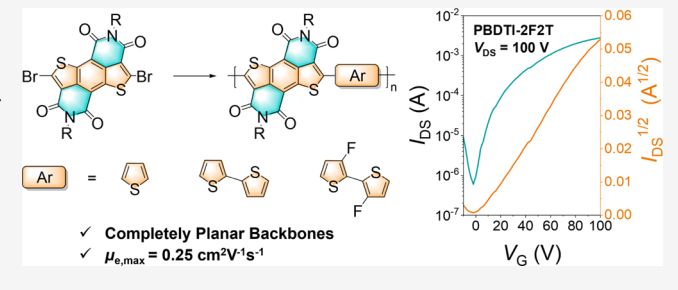
ACCESS I

III Metrics & More

Article Recommendations

sı Supporting Information

ABSTRACT: The research on *p*-type polymer semiconductors has achieved significant progress in terms of material diversity and device performance, while the performance of *n*-type polymer semiconductors has lagged far behind. The design and synthesis of electron-deficient building blocks are essential for the development of high-performance *n*-type polymer semiconductors. Herein, we report a new electron-deficient unit, 3,4,7,8-benzo[1,2-*b*:4,5-*b*']dithiophenedimides (BDTI), and its derivative dibromide BDTI, which are further employed to construct BDTI-based donor—acceptor copolymers. These polymers show highly planar



backbones and deep lowest unoccupied molecular orbital (LUMO) levels (from -3.62 to -3.95 eV), which facilitate electron injection and transport in their thin films. The highest electron mobility of 0.25 cm² V⁻¹ s⁻¹ was achieved in a field-effect transistor (FET) using the copolymer containing a fluorinated bithiophene donor. This work demonstrates that BDTI is a promising building block for constructing high-performance n-type polymer semiconductors.

INTRODUCTION

Conjugated polymer semiconductors have received tremendous attention due to their potential applications in flexible, wearable, and implantable electronic devices. 1-6 Both p-type (hole-transporting) and n-type (electron-transporting) semiconductors are required in practical applications, such as fabricating complementary metal oxide semiconductor (CMOS)-like logic circuits and building bulk heterojunction devices. Nowadays, hole mobilities (μ_h) of p-type polymer semiconductors have exceeded 10 cm² V⁻¹ s⁻¹, which is superior to those of amorphous silicon-based thin film transistors.^{7–9} In comparison, *n*-type polymer semiconductors with high electron mobilities (μ_e) are still limited mainly because of the lack of strong electron-deficient building blocks. 10-15 Thus, the development of novel electron acceptor units and rational polymer structural design is highly required for boosting the performance of n-type polymer semiconductors.

Among the reported electron-deficient units, diimide units such as naphthalene diimide (NDI) and perylene diimide (PDI) have been intensively investigated. $^{16-22}$ On the one hand, two highly electron-withdrawing imide units significantly reduce the LUMO energy levels of diimide-based polymers, promoting electron-transport properties. On the other hand, introducing alkyl groups in the N-positions of imides enables the regulation of the solution processability of diimide-based polymers. However, diimide-based polymers usually exhibit twisted backbones caused by steric crowding of the imide and

adjacent conjugated units.²³⁻²⁵ It is known that twisted backbones may shorten the conjugation length, reduce HOMO/LUMO delocalization, and inhibit polymer-chain stacking, thus limiting charge carrier transporting properties. 26-29 Therefore, to further increase the charge transporting performance, various chemical modifications of diimide-based polymers were carried out to enhance backbone planarity (Scheme 1). One of the straight ways is to introduce π -spacer groups between the diimide unit and comonomer. For instance, Briseno³⁰ and Heeney³¹ independently reported that vinylidene spacers between NDI (NDI-V) and bithiophene moieties could reduce backbone torsion (~18°), and the electron mobility (μ_e) of the resulting conjugated polymers was boosted to 0.28 cm² V⁻¹ s⁻¹. Another strategy is to optimize the structure of the diimide units to reduce steric hindrance. Marks and Facchetti removed one or two carbonyl groups in the NDI units (NBA), and the corresponding polymers exhibited backbone torsion of $\sim 10^{\circ}$ with μ_e of 0.39 cm² V⁻¹ s⁻¹.^{25,32} Li and Guo developed a ring-extended NDI unit, anthracene diimide (ADI), affording polymers that showed backbone torsion of ~11°. 33,34 However, diimide-

Received: May 10, 2024 Revised: June 23, 2024 Accepted: July 4, 2024 Published: July 11, 2024





Scheme 1. Molecular Design Strategies for Enhancing Backbone Planarity of the Diimide-Based Polymers in Previous Reports and This Work

Scheme 2. Synthetic Routes to BDTI and BDTI-Br with Alkyl Chains

based polymers with planar backbones were seldom reported. 35,36

In this paper, we report a new electron-deficient building block, 3,4,7,8-benzo [1,2-b:4,5-b'] dithiophenedimides (BDTI, Scheme 1), by decorating two imides functional group onto benzo[1,2-b:4,5-b']dithiophene (BDT).³⁷ The molecular design is based on the following considerations: (i) the benzo[1,2-b:4,5-b']dithiophene (BDT) possesses expanded conjugation compared to naphthalene, which is the main π conjugated moiety of NDI, and therefore, the intermolecular $\pi - \pi$ interactions in BDTI are expected to be enhanced; (ii) the steric crowding is expected to be reduced by fusing thiophene rings instead of benzene rings, enhancing backbone planarity in BDTI-based polymers; (iii) functional groups such as -Br are easily introduced into the α -position of the thiophene rings. Furthermore, three donor-acceptor (D-A) copolymers were synthesized, PBDTI-T, PBDTI-2T, and PBDTI-2F2T, in which BDTI serves as the electron acceptor unit, thiophene (T), 2,2'-bithiophene (2T), and 3,3'-difluoro-2,2'-bithiophene (2F2T) as the respective electron donor units. All three polymers exhibit nearly planar backbones and relatively high electron mobilities up to 0.25 cm² V⁻¹ s⁻¹ in bottom-gate/bottom-contact FETs.

■ RESULTS AND DISCUSSION

The synthesis of BDTI and its derivatives is shown in Scheme 2, with details reported in the Supporting Information. Diethyl

benzo[1,2-b:4,5-b']dithiophene-4,8-dicarboxylate 1 was treated with KOH in dioxane/water to yield the corresponding dicarboxylic acid 2, which was further reacted with thionyl chloride, producing dicarbonyl dichloride compound 3. Next, compound 3 was reacted with hexyl isocyanate through a Lewis acid-mediated Friedel-Crafts cyclization to obtain the desired compound C6-BDTI, for which the possible reaction mechanism is illustrated in Scheme S1. To serve as a building block, dibrominated BDTI derivatives (BDTI-Br) are needed. However, direct bromination of C6-BDTI failed, probably due to the strong electron-withdrawing property of imide units, reducing the reactivity of thiophene rings. Instead, a prebromination route was selected. Bromination of starting compound 1 with liquid bromine yielded the dibrominated compound 4, followed by similar ester hydrolysis, acylation, and Friedel-Crafts cyclization to afford C6-BDTI-Br and 4octyltetradecyl-substituted BDTI-Br (4-OT-BDTI-Br). The chemical structures of BDTI and BDTI-Br were characterized by NMR, high-resolution mass spectrometry (HRMS), and elemental analysis.

The crystal structure of C6-BDTI was successfully determined. As shown in Figure 1a, the conjugated skeleton of C6-BDTI is fully planar. The intramolecular S···O distance in C6-BDTI is 3.03 Å, shorter than the sum of van der Waals radii of S and O atoms (1.84 and 1.40 Å). Such S···O noncovalent interactions are expected to further enhance the planarity of the BDTI core. 38,39 In the crystal lattice, molecules

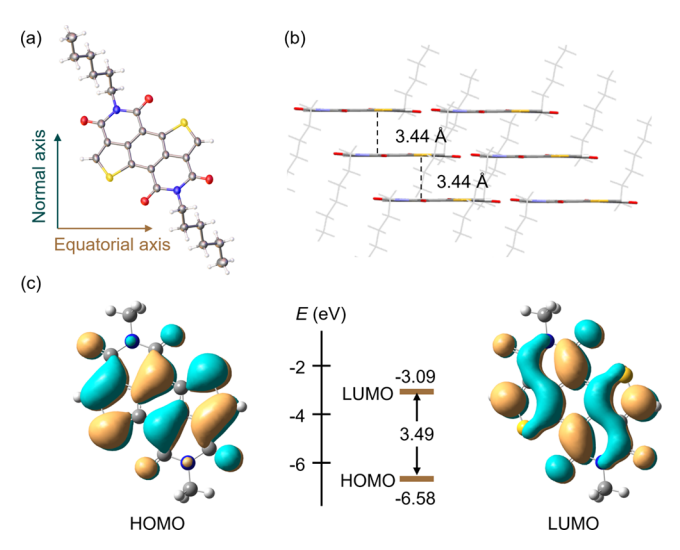


Figure 1. (a) Crystal structure and (b) intermolecular packing of C6-BDTI. (c) DFT-calculated frontier molecular orbital (FMO) energies and FMO isosurface (the isosurface value is 0.02) of C6-BDTI, in which the hexyl groups were replaced with methyl groups.

of C6-BDTI adopt a one-dimensional slipped stacked packing motif with a short π – π stacking distance of 3.44 Å (Figure 1b). The highly planar core and close π – π stacking distance are beneficial for efficient charge transport properties.

The LUMO energy of C6-BDTI was estimated to be -3.55eV, based on the onset of the first reduction wave obtained from the cyclic voltammogram (Figure S2). The LUMO energy of C6-BDTI is slightly higher than that of NDI⁴⁰ due to the electron-donating nature of thiophene moieties. The optical bandgap was estimated to be 2.79 eV, according to the onset absorption in the UV-vis absorption spectrum of C6-BDTI thin film (Figure S3). Therefore, the HOMO energy of C6-BDTI was calculated to be -6.34 eV. To further investigate the electronic properties of the BDTI core, density functional theory (DFT) calculations were carried out at the $B3LYP-D3(BJ)/6-31G^{**}$ level of theory, in which the N-alkyl chains are replaced by N-methyl groups. The HOMO of BDTI is mainly delocalized along the equatorial axis, while its LUMO is mainly delocalized along the normal axis (Figure 1c). The relatively low LUMO energy levels and orbital delocalization of the BDTI core enable it to be a promising electron acceptor unit for *n*-type polymer semiconductors.

The BDTI-based polymers PBDTI-T, PBDTI-2T, and PBDTI-2F2T (Scheme 3) were synthesized via Stille cross-coupling of branched alkyl-substituted 4-OT-BDTI-Br with

2,5-bis(trimethylstannyl)thiophene, 5,5'-bis(trimethylstannyl)-2,2'bithiophene, and (3,3'-difluoro-[2,2'-bithiophene]-5,5'diyl)bis(trimethylstannane), respectively, in 64, 87, and 82% yields. The utilization of the branched alkyl-substituted 4-OT-BDTI-Br is to ensure the solubility of the resulting polymers. These polymers show good solubility in common organic solvents, such as chloroform, toluene, and chlorobenzene. High-temperature (160 °C) gel permeating chromatography (GPC) was used to measure the molecular weights of the BDTI-based polymers. The resulting number-average molecular weights (M_n) of PBDTI-T, PBDTI-2T, and PBDTI-2F2T were 12.3, 58.4, and 21.8 kDa, respectively, with the polydispersity indexes (PDI) of 1.7, 3.3, and 2.6 (Figure S4 and Table 1). All these polymers exhibit excellent thermal stability, with onset decomposition temperatures over 400 °C as measured by thermogravimetric analysis (TGA, Figure S5a). Their thermal behaviors were also characterized in the range from 25 to 350 °C by differential scanning calorimetry (DSC, Figure S5b). During the heating and cooling processes, no obvious phase transition was observed for the three polymers, which is a common phenomenon in rigid π -conjugated polymers.41,42

Figure 2a,b shows the absorption spectra of BDTI-based polymers in chloroform and their thin films. The solutions of three BDTI-based polymers exhibit strong absorptions in the range 500-800 nm and weak absorptions in the range 300-500 nm (Figure 2a). Specifically, PBDTI-T, PBDTI-2T, and PBDTI-2F2T in chloroform absorb strongly around 698/657, 745/687, and 731/679 nm, respectively. This is significantly different from the absorption spectrum of N2200, the NDIbased n-type polymer semiconductor, which displays a strong absorption band in the range of 300-500 nm and a weak absorption band in the range of 500-800 nm. 20,43 This result may be due to the reduced steric crowding effects of the BDTIbased polymers, which enhance the degree of conjugation of the conjugated backbone. As shown in Figure 2b, thin films of three BDTI-based polymers show similar absorption spectra with strong absorptions in the range of 500-800 nm. In comparison with those of BDTI-based polymers in solution, the absorption spectra of their thin films are only slightly redshifted. This may be ascribed to the occurrence of the preaggregation of BDTI-based polymers in their solutions. Based on the onset absorptions of their thin films, the optical energy bandgaps of PBDTI-T, PBDTI-2T, and PBDTI-2F2T were estimated to be 1.56, 1.51, and 1.50 eV, respectively.

The electrochemical properties of BDTI-based polymer films are measured with cyclic voltammetry and are summarized in Table 1. Based on the onsets of the first

Scheme 3. Synthetic Routes to BDTI-Based Polymers

Table 1. Molecular Weights, Maximum Absorption Peaks, and HOMO/LUMO Energies of BDTI-Based Polymers

polymer	$M_{\rm n}~({\rm kDa})$	PDI	$\lambda_{\max}^{\text{sol.}}$ (nm)	$\lambda_{\max}^{\text{film}}$ (nm)	$E_{\rm gap}^{\rm \ opt} \ ({\rm eV})$	E_{LUMO} (eV)	E_{HOMO} (eV)
PBDTI-T	12.3	1.7	698/657	705/662	1.56	-3.95	-5.51
PBDTI-2T	58.4	3.3	745/687	736/685	1.50	-3.62	-5.12
PBDTI-2F2T	21.8	2.6	731/679	728/681	1.51	-3.76	-5.27

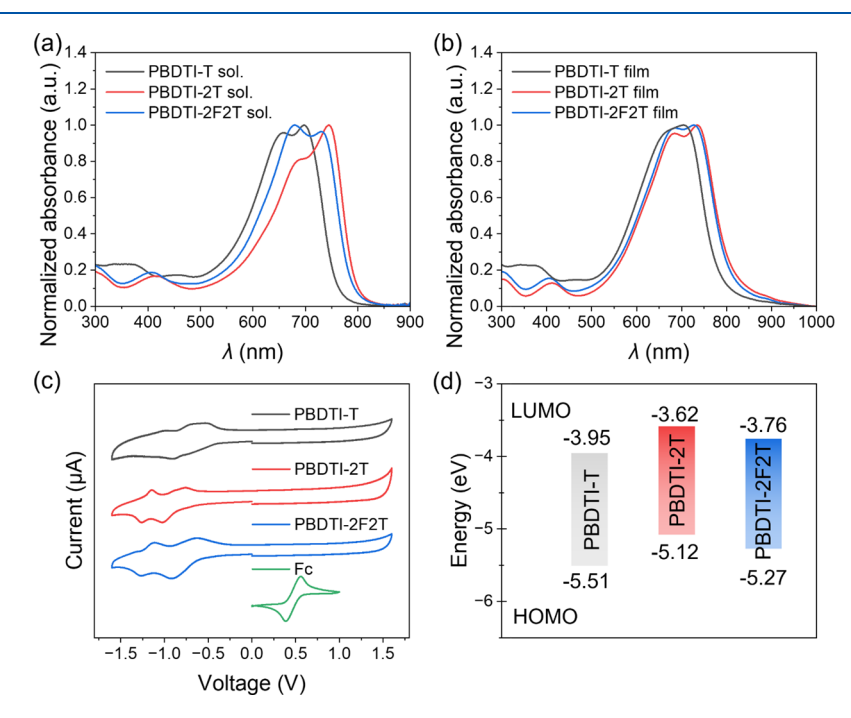


Figure 2. Absorption spectra of (a) solutions of PBDTI-T, PBDTI-2T, and PBDTI-2F2T in chloroform and (b) their thin films. (c) Cyclic voltammograms and (d) FMO energy diagram of BDTI-based polymers, $E_{\text{LUMO}} = -(E_{\text{red}}^{\text{onset}} + 4.8 - E_{\text{ox}}^{\text{Fc/Fc+}})$ eV, $E_{\text{ox}}^{\text{Fc/Fc+}} = 0.44$ eV, $E_{\text{HOMO}} = E_{\text{LUMO}} - E_{\text{gap}}^{\text{opt}}$, $E_{\text{gap}}^{\text{opt}} = (1240/\lambda_{\text{onset}})$ eV.

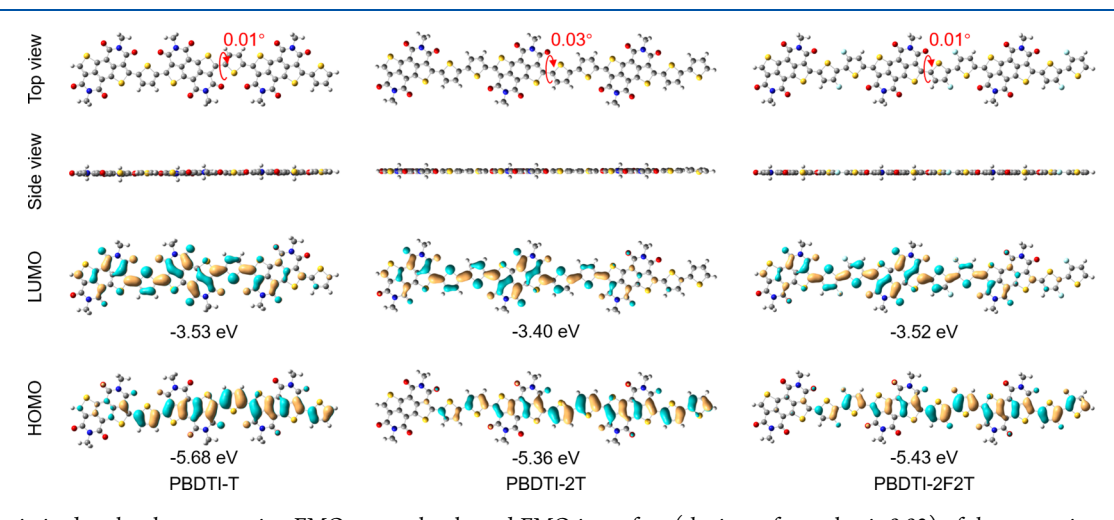


Figure 3. Optimized molecular geometries, FMO energy levels, and FMO isosurface (the isosurface value is 0.02) of the respective repeat units of the BDTI-based polymers computed at the B3LYP-D3(BJ)/6-31G** level of theory; the alkyl chains were replaced with methyl groups.

reduction waves, the LUMO energies of PBDTI-T, PBDTI-2T, and PBDTI-2F2T were estimated to be -3.95, -3.62, and -3.76 eV, respectively. From their optical bandgaps and LUMO energies, the HOMO energies of PBDTI-T, PBDTI-2T, and PBDTI-2F2T were estimated to be -5.51, -5.12, and -5.27 eV, respectively (Figure 2c,d). These data suggest that these BDTI-based polymers exhibit low LUMO energies and can potentially function as n-type polymer semiconductors.

We also performed DFT calculations on the three repeat units of PBDTI-T, PBDTI-2T, and PBDTI-2F2T to further understand their backbone conformations and electronic structures. As shown in Figure 3, all three BDTI-based polymers show almost completely planar backbones, which should have originated from the small steric hindrance of BDTI, as well as the intramolecular noncovalent S···O interactions of the BDTI and thiophene moieties. Moreover, the HOMOs and LUMOs of three BDTI-based polymers are

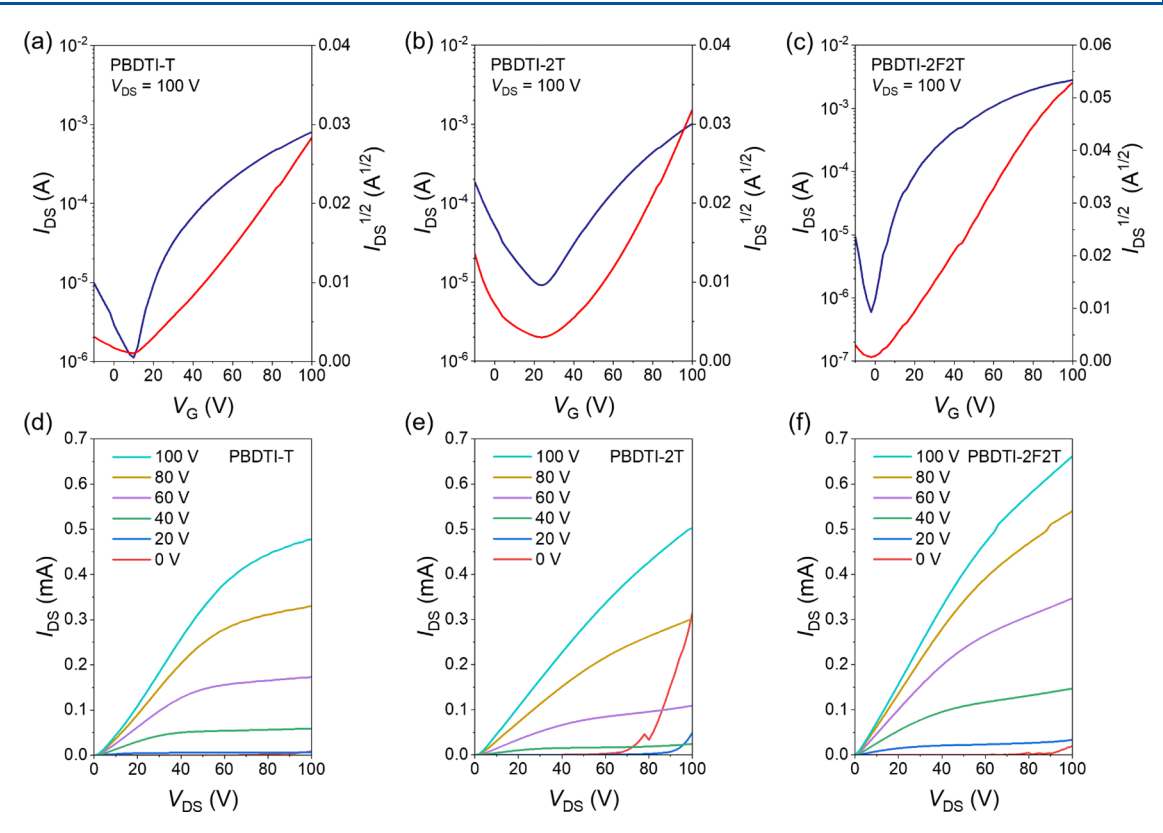


Figure 4. (a-c) Transfer and (d-f) output curves of BGBC FET devices using (a, d) PBDTI-T, (b, e) PBDTI-2T, and (c, f) PBDTI-2F2T as active layers.

distributed almost over their backbones; thus, they present delocalized orbital wave functions. The calculated HOMO/LUMO energies of PBDTI-T, PBDTI-2T, and PBDI-2F2T are consistent with the trend in experimental results. These new polymers with planar backbones and delocalized orbital wave functions will enable efficient intermolecular interactions and uniform solid-state organizations, thereby facilitating electron carrier transport.

The semiconducting properties of these BDTI-based polymers were evaluated by fabricating bottom-gate/bottom-contact (BGBC) FET devices under an inert atmosphere. Figure 4 shows the representative transfer and output curves of the devices with PBDTI-T, PBDTI-2T, and PBDTI-2F2T as the respective semiconducting layers. Clearly, thin films of PBDTI-2F2T show *n*-type semiconducting behavior, while a thin film of PBDTI-2T behaves as an ambipolar semiconductor. The semiconducting performance parameters were extracted and are listed in Table 2. As expected, the device performance was also affected by the thermal annealing of thin films of BDTI-based polymers (Figures S7 and S8, Table S3). Among thin films of BDTI-based polymers, the thin film of PBDTI-2F2T exhibits the best *n*-type transporting property with the maximum/average electron mobility of 0.25/

Table 2. FET Performance Parameters of the BDTI-Based Polymers

polymer	T_{anneal} (°C)	$\mu_{\rm e,av}^{a} ({\rm cm}^2 {\rm V}^{-1} {\rm S}^{-1})$	V_{th} (V)	$I_{\rm ON}/I_{\rm OFF}$
PBDTI-T	250	0.059	10-15	$10^3 - 10^4$
PBDTI-2T	250	0.15	36-40	$10^1 - 10^2$
PBDTI-2F2T	250	0.22	11-20	$10^3 - 10^4$

^aAverage values from five devices.

0.22 cm² V⁻¹ s⁻¹ after being annealed at 250 °C for 10 min (Figure 4c,f). The device with PBDTI-T also shows *n*-type transporting characteristics, which agrees with the fact that PBDTI-T possesses the lowest LUMO energy among the three polymers. However, the device exhibits low electron mobility with an average $\mu_{\rm e}$ of 0.059 cm² V⁻¹ s⁻¹ (Figure 4a,d). This may be attributed to its relatively poor film crystallinity as it will be discussed below. In comparison, a thin film of PBDTI-2T without fluorine substituents shows ambipolar characteristics with an average $\mu_{\rm e}$ of 0.15 cm 2 V $^{-1}$ s $^{-1}$ and an average $\mu_{\rm h}$ of 0.17 cm² V⁻¹ s⁻¹ based on the transfer and output curves (Figures 4b,e and S9). The difference between PBDTI-2F2T and PBDTI-2T may be attributed to the stronger electrondonating properties of bithiophene, which results in the appearance of p-type performance and the suppression of ntype characteristics for PBDTI-2T.

To understand the difference in the charge-transport properties of the three polymers, the morphologies and microstructures of the pristine and annealed films were characterized with atomic force microscopy (AFM) and grazing incidence wide-angle X-ray scattering (GIWAXS). Compared with the pristine polymer films, the RMS values of annealed polymer films increased, and the diffraction peaks became more pronounced, demonstrating the positive effect of thermal annealing on increasing polymer packing of polymer chains (Figures 5 and S10). The AFM height images indicated that all annealed BDTI-based polymer films show smooth surfaces with small root-mean-square (RMS) roughness values of 0.71, 1.46, and 1.67 nm for PBDTI-T, PBDTI-2T, and PBDTI-2F2T, respectively (Figure 5a-c). The two-dimensional (2D) GIWAXS plots and the corresponding in-plane and out-of-plane line cuts are shown in Figures 5d-f and S11,

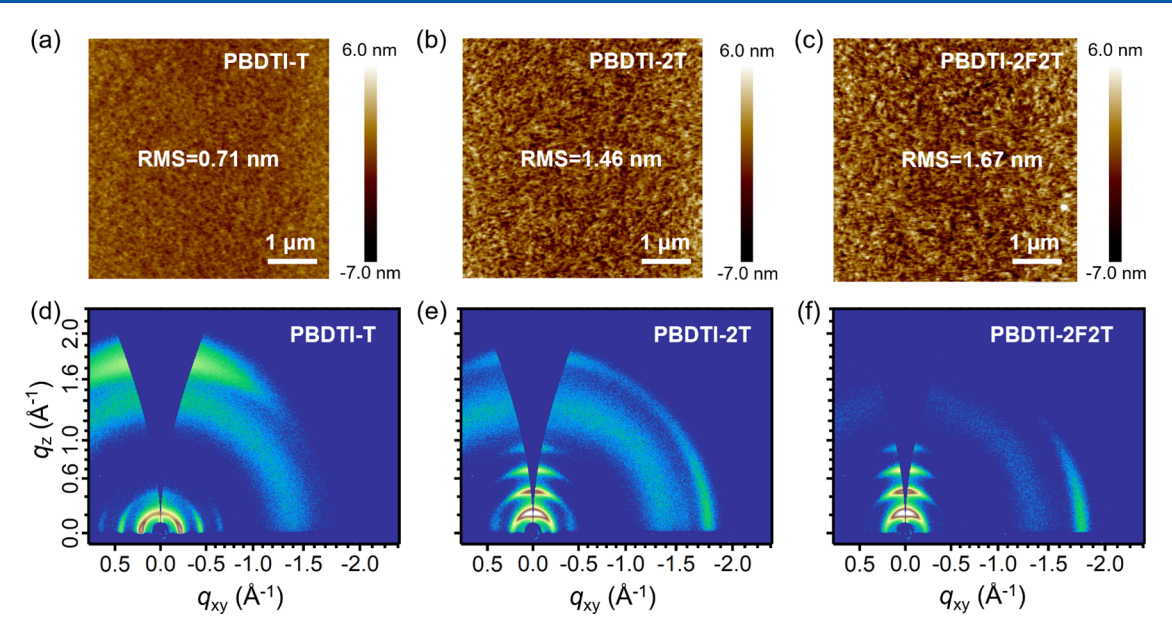


Figure 5. AFM height images and GIWAXS patterns of the thermally annealed BDTI-based polymer films: (a, d) PBDTI-T, (b, e) PBDTI-2T, and (c, f) PBDTI-2F2T.

respectively. The three annealed BDTI-based polymer thin films showed different diffraction characteristics. For PBDTI-T thin film, the lamellar stacking (h00) signals are seen in the inplane direction, and the $\pi-\pi$ stacking peak (010) appears in the out-of-plane direction, indicating that polymer chains adopt the face-on packing model on the surface. For the PBDTI-2T thin film, strong lamellar stacking signals are detected in the out-of-plane direction. However, the (010) peak (albeit weak) is observed in both in-plane and out-of-plane directions. Thus, polymer chains of PBDTI-2T are orientated on the surface in both face-on and edge-on models. For the PBDTI-2F2T thin film, more pronounced (h00) diffraction peaks are observable in the out-of-plane direction, and an obvious (010) peak is also detected in the in-plane direction, indicating that polymer chains of PBDTI-2F2T are edge-on packed on the surface. The edge-on packing model has been proven to facilitate charge transport in FET devices. 44,45 According to the (100) signals, the three polymer thin films show similar layer stacking distances of approximately 28.29 Å, while from the (010) diffraction peak, the π - π stacking distance varies from 3.60 Å for PBDTI-T to 3.51 Å for PBDTI-2T and to 3.49 Å for PBDTI-2F2T. Moreover, the coherence lengths of these three polymer films were estimated based on the full width at halfmaximum (fwhm) of the respective (100) peaks using the Scherrer equation.³ The coherence lengths of PBDTI-T, PBDTI-2T, and PBDTI-2F2T were calculated to be 165.26, 251.20, and 273.04 Å (Table S4), respectively. Therefore, the fact that the thin film of PBDTI-2F2T exhibits the best electron-transport performance can be attributed to the high thin film crystallinity with large coherence length and the interchain edge-on packing with short π – π stacking distance.

CONCLUSIONS

In summary, we report a new electron-deficient building block (BDTI) via Lewis-acid-mediated Friedel—Crafts cyclization of acid chlorides and isocyanates. The BDTI unit shows a rigid and highly planar skeleton with a short $\pi-\pi$ stacking distance of 3.44 Å, as illustrated by a single-crystal structural analysis. By copolymerizing BDTI acceptor units with three electron

donors (thiophene, bithiophene, and difluorobithiophene) separately, three D-A type polymers (PBDTI-T, PBDTI-2T, and PBDTI-2F2T) were prepared with the lowest LUMO energy of -3.95 eV. DFT calculations indicate that backbone torsion of BDTI-based polymers is significantly suppressed compared to the corresponding NDI-based polymer due to the small steric hindrance of BDTI. The low LUMO energy and almost planar backbone of these polymers facilitate electron injection and transport. Among them, the thin film of PBDTI-2F2T shows the highest electron mobility of $0.25 \text{ cm}^2 \text{ V}^{-1} \text{ s}^{-1}$, attributed to the high thin film crystallinity and edge-on orientation of polymer chains. These results demonstrate that BDTI is a promising building block for constructing highperformance n-type polymer semiconductors, and the functionalization of arenes by incorporating diimide units is a powerful strategy for developing strongly electron-deficient units for high-performance organic optoelectronic materials.

ASSOCIATED CONTENT

Supporting Information

The Supporting Information is available free of charge at https://pubs.acs.org/doi/10.1021/acs.macromol.4c01064.

Materials and methods, synthesis and characterizations, device fabrication and measurements, thin film morphology analysis, and NMR spectra (PDF)

AUTHOR INFORMATION

Corresponding Author

Deqing Zhang — Beijing National Laboratory for Molecular Sciences, CAS Key Laboratory of Organic Solids, Institute of Chemistry, Chinese Academy of Sciences, Beijing 100190, P. R. China; University of Chinese Academy of Sciences, Beijing 100049, P. R. China; ⊚ orcid.org/0000-0002-5709-6088; Email: dqzhang@iccas.ac.cn

Authors

Zhichun Shangguan — Beijing National Laboratory for Molecular Sciences, CAS Key Laboratory of Organic Solids,

- Institute of Chemistry, Chinese Academy of Sciences, Beijing 100190, P. R. China; orcid.org/0000-0003-0517-0677
- Zheng Yin Beijing National Laboratory for Molecular Sciences, CAS Key Laboratory of Organic Solids, Institute of Chemistry, Chinese Academy of Sciences, Beijing 100190, P. R. China
- Cheng Li − Beijing National Laboratory for Molecular Sciences, CAS Key Laboratory of Organic Solids, Institute of Chemistry, Chinese Academy of Sciences, Beijing 100190, P. R. China; orcid.org/0000-0001-9377-9049
- Wansong Shang Beijing National Laboratory for Molecular Sciences, CAS Key Laboratory of Organic Solids, Institute of Chemistry, Chinese Academy of Sciences, Beijing 100190, P. R. China
- Liangliang Chen Beijing National Laboratory for Molecular Sciences, CAS Key Laboratory of Organic Solids, Institute of Chemistry, Chinese Academy of Sciences, Beijing 100190, P. R. China
- Chenying Gao Beijing National Laboratory for Molecular Sciences, CAS Key Laboratory of Organic Solids, Institute of Chemistry, Chinese Academy of Sciences, Beijing 100190, P. R. China; University of Chinese Academy of Sciences, Beijing 100049, P. R. China
- Xiang Xue Beijing National Laboratory for Molecular Sciences, CAS Key Laboratory of Organic Solids, Institute of Chemistry, Chinese Academy of Sciences, Beijing 100190, P. R. China; University of Chinese Academy of Sciences, Beijing 100049, P. R. China
- Xisha Zhang Beijing National Laboratory for Molecular Sciences, CAS Key Laboratory of Organic Solids, Institute of Chemistry, Chinese Academy of Sciences, Beijing 100190, P. R. China; University of Chinese Academy of Sciences, Beijing 100049, P. R. China
- Guanxin Zhang Beijing National Laboratory for Molecular Sciences, CAS Key Laboratory of Organic Solids, Institute of Chemistry, Chinese Academy of Sciences, Beijing 100190, P. R. China; orcid.org/0000-0002-1417-6985

Complete contact information is available at: https://pubs.acs.org/10.1021/acs.macromol.4c01064

Notes

The authors declare no competing financial interest.

ACKNOWLEDGMENTS

This work was partially supported by NSFC (22322507, 22075293, 22021002, and 22090021), the Chinese Academy of Sciences (XDB0520000, GJTD-2020-02), and the Beijing Municipal Natural Science Foundation (Z220025). This work was also supported by the Youth Innovation Promotion Association CAS (No. 2022031).

REFERENCES

- (1) Ding, L.; Yu, Z. D.; Wang, X. Y.; Yao, Z. F.; Lu, Y.; Yang, C. Y.; Wang, J. Y.; Pei, J. Polymer Semiconductors: Synthesis, Processing, and Applications. *Chem. Rev.* **2023**, *123*, 7421–7497.
- (2) Qiu, Z.; Hammer, B. A. G.; Müllen, K. Conjugated polymers Problems and promises. *Prog. Polym. Sci.* **2020**, *100*, No. 101179.
- (3) Yu, X.; Chen, L.; Li, C.; Gao, C.; Xue, X.; Zhang, X.; Zhang, G.; Zhang, D. Intrinsically Stretchable Polymer Semiconductors with Good Ductility and High Charge Mobility through Reducing the Central Symmetry of the Conjugated Backbone Units. *Adv. Mater.* 2023, 35, No. 2209896.

- (4) Zhang, D.; Li, C.; Zhang, G.; Tian, J.; Liu, Z. Phototunable and Photopatternable Polymer Semiconductors. *Acc. Chem. Res.* **2024**, *57*, 625–635.
- (5) Zheng, Y.; Zhang, S.; Tok, J. B. H.; Bao, Z. Molecular Design of Stretchable Polymer Semiconductors: Current Progress and Future Directions. *J. Am. Chem. Soc.* **2022**, *144*, 4699–4715.
- (6) Park, K. S.; Kwok, J. J.; Dilmurat, R.; Qu, G.; Kafle, P.; Luo, X.; Jung, S.-H.; Olivier, Y.; Lee, J.-K.; Mei, J.; Beljonne, D.; Diao, Y. Tuning conformation, assembly, and charge transport properties of conjugated polymers by printing flow. *Sci. Adv.* **2019**, *S*, No. eaaw7757.
- (7) Tseng, H.-R.; Phan, H.; Luo, C.; Wang, M.; Perez, L. A.; Patel, S. N.; Ying, L.; Kramer, E. J.; Nguyen, T.-Q.; Bazan, G. C.; Heeger, A. J. High-Mobility Field-Effect Transistors Fabricated with Macroscopic Aligned Semiconducting Polymers. *Adv. Mater.* **2014**, *26*, 2993–2998.
- (8) Ji, Y.; Xiao, C.; Wang, Q.; Zhang, J.; Li, C.; Wu, Y.; Wei, Z.; Zhan, X.; Hu, W.; Wang, Z.; Janssen, R. A. J.; Li, W. Asymmetric Diketopyrrolopyrrole Conjugated Polymers for Field-Effect Transistors and Polymer Solar Cells Processed from a Nonchlorinated Solvent. *Adv. Mater.* **2016**, 28, 943–950.
- (9) Yao, J.; Yu, C.; Liu, Z.; Luo, H.; Yang, Y.; Zhang, G.; Zhang, D. Significant Improvement of Semiconducting Performance of the Diketopyrrolopyrrole—Quaterthiophene Conjugated Polymer through Side-Chain Engineering via Hydrogen-Bonding. *J. Am. Chem. Soc.* **2016**, *138*, 173–185.
- (10) Zhang, Y.; Wang, Y.; Gao, C.; Ni, Z.; Zhang, X.; Hu, W.; Dong, H. Recent advances in n-type and ambipolar organic semiconductors and their multi-functional applications. *Chem. Soc. Rev.* **2023**, *52*, 1331–1381.
- (11) Cao, X.; Li, H.; Hu, J.; Tian, H.; Han, Y.; Meng, B.; Liu, J.; Wang, L. An Amorphous n-Type Conjugated Polymer with an Ultra-Rigid Planar Backbone. *Angew. Chem., Int. Ed.* **2023**, 62, No. e202212979.
- (12) Feng, K.; Guo, H.; Sun, H.; Guo, X. n-Type Organic and Polymeric Semiconductors Based on Bithiophene Imide Derivatives. *Acc. Chem. Res.* **2021**, *54*, 3804–3817.
- (13) Meng, J.; Dou, J.; Zhou, Z.; Chen, P.; Luo, N.; Li, Y.; Luo, L.; He, F.; Geng, H.; Shao, X.; Zhang, H.-L.; Liu, Z. Non-symmetric Half-Fused BN Coordinated Diketopyrrolopyrrole Building Block for n-type Semiconducting Polymers. *Angew. Chem., Int. Ed.* **2023**, *62*, No. e202301863.
- (14) Yang, J.; Li, J.; Zhang, X.; Yang, W.; Jeong, S. Y.; Huang, E.; Liu, B.; Woo, H. Y.; Chen, Z.; Guo, X. Functionalized Phenanthrene Imide-Based Polymers for n-Type Organic Thin-Film Transistors. *Angew. Chem., Int. Ed.* **2024**, *63*, No. e202319627.
- (15) Shen, T.; Li, W.; Zhao, Y.; Wang, Y.; Liu, Y. A Hybrid Acceptor-Modulation Strategy: Fluorinated Triple-Acceptor Architecture for Significant Enhancement of Electron Transport in High-Performance Unipolar n-Type Organic Transistors. *Adv. Mater.* 2023, 35, No. 2210093.
- (16) Wang, Y.; Hasegawa, T.; Matsumoto, H.; Michinobu, T. Significant Improvement of Unipolar n-Type Transistor Performances by Manipulating the Coplanar Backbone Conformation of Electron-Deficient Polymers via Hydrogen Bonding. J. Am. Chem. Soc. 2019, 141, 3566–3575.
- (17) Cheng, P.; Zhao, X.; Zhan, X. Perylene Diimide-Based Oligomers and Polymers for Organic Optoelectronics. *Acc. Mater. Res.* **2022**, *3*, 309–318.
- (18) Yuan, Z.; Buckley, C.; Thomas, S.; Zhang, G.; Bargigia, I.; Wang, G.; Fu, B.; Silva, C.; Brédas, J.-L.; Reichmanis, E. A Thiazole—Naphthalene Diimide Based n-Channel Donor—Acceptor Conjugated Polymer. *Macromolecules* **2018**, *51*, 7320—7328.
- (19) Chen, Z.; Zheng, Y.; Yan, H.; Facchetti, A. Naphthalenedicarboximide- vs perylenedicarboximide-based copolymers. Synthesis and semiconducting properties in bottom-gate N-channel organic transistors. *J. Am. Chem. Soc.* **2009**, *131*, 8–9.
- (20) Guo, X.; Watson, M. D. Conjugated polymers from naphthalene bisimide. *Org. Lett.* **2008**, *10*, 5333–5336.

- (21) Zhan, X.; Tan, Z.; Domercq, B.; An, Z.; Zhang, X.; Barlow, S.; Li, Y.; Zhu, D.; Kippelen, B.; Marder, S. R. A high-mobility electron-transport polymer with broad absorption and its use in field-effect transistors and all-polymer solar cells. *J. Am. Chem. Soc.* **2007**, *129*, 7246–7247.
- (22) Xin, H.; Hou, B.; Gao, X. Azulene-Based π -Functional Materials: Design, Synthesis, and Applications. *Acc. Chem. Res.* **2021**, *54*, 1737–1753.
- (23) Sun, H.; Guo, X.; Facchetti, A. High-Performance n-Type Polymer Semiconductors: Applications Recent Development, and Challenges. *Chem.* **2020**, *6*, 1310–1326.
- (24) Li, Y.; Huang, E.; Guo, X.; Feng, K. Cyano-functionalized organic and polymeric semiconductors for high-performance n-type organic electronic devices. *Mater. Chem. Front.* **2023**, *7*, 3803–3819.
- (25) Chen, Y.; Wu, J.; Lu, S.; Facchetti, A.; Marks, T. J. Semiconducting Copolymers with Naphthalene Imide/Amide pi-Conjugated Units: Synthesis, Crystallography, and Systematic Structure-Property-Mobility Correlations. *Angew. Chem., Int. Ed.* **2022**, *61*, No. e202208201.
- (26) Zhu, C.; Kalin, A. J.; Fang, L. Covalent and Noncovalent Approaches to Rigid Coplanar π-Conjugated Molecules and Macromolecules. *Acc. Chem. Res.* **2019**, *52*, 1089–1100.
- (27) Alsufyani, M.; Stoeckel, M.-A.; Chen, X.; Thorley, K.; Hallani, R. K.; Puttisong, Y.; Ji, X.; Meli, D.; Paulsen, B. D.; Strzalka, J.; Regeta, K.; Combe, C.; Chen, H.; Tian, J.; Rivnay, J.; Fabiano, S.; McCulloch, I. Lactone Backbone Density in Rigid Electron-Deficient Semiconducting Polymers Enabling High n-type Organic Thermoelectric Performance. *Angew. Chem., Int. Ed.* **2022**, *61*, No. e202113078.
- (28) Prodhan, S.; Qiu, J.; Ricci, M.; Roscioni, O. M.; Wang, L.; Beljonne, D. Design Rules to Maximize Charge-Carrier Mobility along Conjugated Polymer Chains. *J. Phys. Chem. Lett.* **2020**, *11*, 6519–6525.
- (29) Fratini, S.; Nikolka, M.; Salleo, A.; Schweicher, G.; Sirringhaus, H. Charge transport in high-mobility conjugated polymers and molecular semiconductors. *Nat. Mater.* **2020**. *19*. 491–502.
- (30) Zhang, L.; Rose, B. D.; Liu, Y.; Nahid, M. M.; Gann, E.; Ly, J.; Zhao, W.; Rosa, S. J.; Russell, T. P.; Facchetti, A.; McNeill, C. R.; Brédas, J.-L.; Briseno, A. L. Efficient Naphthalenediimide-Based Hole Semiconducting Polymer with Vinylene Linkers between Donor and Acceptor Units. *Chem. Mater.* **2016**, *28*, 8580–8590.
- (31) Fei, Z.; Han, Y.; Martin, J.; Scholes, F. H.; Al-Hashimi, M.; AlQaradawi, S. Y.; Stingelin, N.; Anthopoulos, T. D.; Heeney, M. Conjugated Copolymers of Vinylene Flanked Naphthalene Diimide. *Macromolecules* **2016**, *49*, 6384–6393.
- (32) Eckstein, B. J.; Melkonyan, F. S.; Manley, E. F.; Fabiano, S.; Mouat, A. R.; Chen, L. X.; Facchetti, A.; Marks, T. J. Naphthalene Bis(4,8-diamino-1,5-dicarboxyl)amide Building Block for Semiconducting Polymers. *J. Am. Chem. Soc.* **2017**, *139*, 14356–14359.
- (33) Tu, D.; Yang, Q.; Yu, S.; Guo, X.; Li, C. Isomeric anthracene diimide polymers. *Chem. Sci.* **2021**, *12*, 2848–2852.
- (34) Tu, D.; Feng, Z.; Feng, Z.; Guo, X.; Li, C. Crystallinity and Orientation Manipulation of Anthracene Diimide Polymers for All-Polymer Solar Cells. *Adv. Funct. Mater.* **2021**, 31, No. 2011049.
- (35) Fukutomi, Y.; Nakano, M.; Hu, J. Y.; Osaka, I.; Takimiya, K. Naphthodithiophenediimide (NDTI): synthesis, structure, and applications. *J. Am. Chem. Soc.* **2013**, *135*, 11445–11448.
- (36) Usta, H.; Newman, C.; Chen, Z.; Facchetti, A. Dithienocoronenediimide-based copolymers as novel ambipolar semiconductors for organic thin-film transistors. *Adv. Mater.* **2012**, *24*, 3678–3684.
- (37) An, C.; Hou, J. Benzo[1,2-b:4,5-b']dithiophene-Based Conjugated Polymers for Highly Efficient Organic Photovoltaics. *Acc. Mater. Res.* **2022**, *3*, 540–551.
- (38) Liu, M.; Han, X.; Chen, H.; Peng, Q.; Huang, H. A molecular descriptor of intramolecular noncovalent interaction for regulating optoelectronic properties of organic semiconductors. *Nat. Commun.* **2023**, *14*, 2500.

- (39) Zhang, X.; Gu, X.; Huang, H. Low-Cost Nonfused-Ring Electron Acceptors Enabled by Noncovalent Conformational Locks. *Acc. Chem. Res.* **2024**, *57*, 981–991.
- (40) Bhosale, S. V.; Al Kobaisi, M.; Jadhav, R. W.; Morajkar, P. P.; Jones, L. A.; George, S. Naphthalene diimides: perspectives and promise. *Chem. Soc. Rev.* **2021**, *50*, 9845–9998.
- (41) Chen, Z.; Li, J.; Wang, J.; Yang, K.; Zhang, J.; Wang, Y.; Feng, K.; Li, B.; Wei, Z.; Guo, X. Imide-Functionalized Fluorenone and Its Cyanated Derivative Based n-Type Polymers: Synthesis, Structure—Property Correlations, and Thin-Film Transistor Performance. *Angew. Chem., Int. Ed.* **2022**, *61*, No. e202205315.
- (42) Xie, R.; Weisen, A. R.; Lee, Y.; Aplan, M. A.; Fenton, A. M.; Masucci, A. E.; Kempe, F.; Sommer, M.; Pester, C. W.; Colby, R. H.; Gomez, E. D. Glass transition temperature from the chemical structure of conjugated polymers. *Nat. Commun.* **2020**, *11*, 893.
- (43) Yan, H.; Chen, Z.; Zheng, Y.; Newman, C.; Quinn, J. R.; Dotz, F.; Kastler, M.; Facchetti, A. A high-mobility electron-transporting polymer for printed transistors. *Nature* **2009**, *457*, 679–686.
- (44) Jiang, Y.; Chen, J.; Sun, Y.; Li, Q.; Cai, Z.; Li, J.; Guo, Y.; Hu, W.; Liu, Y. Fast Deposition of Aligning Edge-On Polymers for High-Mobility Ambipolar Transistors. *Adv. Mater.* **2019**, *31*, No. 1805761.
- (45) Schuettfort, T.; Thomsen, L.; McNeill, C. R. Observation of a Distinct Surface Molecular Orientation in Films of a High Mobility Conjugated Polymer. *J. Am. Chem. Soc.* **2013**, *135*, 1092–1101.